INSTITUTE OF PLASMA PHYSICS

NAGOYA UNIVERSITY

RESEARCH REPORT

NAGOYA, JAPAN

Extraction of a Long-Pulsed Intense Electron Beam from a Pulsed Plasma based on Hollow Cathode Discharge

Johshin Uramoto

IPPJ-288 May 1977

Further communication about this report is to be sent to the Research Information Center, Institute of Plasma Physics, Nagoya University, Nagoya, Japan.

Abstract

An intense electron beam (up to 1.0 kV, 0.8 kA in 0.8 cmϕ) is extracted along a uniform magnetic field with a long decay time (up to 2 msec) from a pulsed high density plasma source which is produced with a fast rise time (< 100 μsec) by a secondary discharge based on a dc hollow cathode discharge. Through a back stream of ionized ions from a beam-extracting anode region where a neutral gas is fed, a space charge limit of the electron beam is so reduced that the beam current is determined by an initially injected electron flux and concentrated in a central aperture of the extracting anode. Moreover, the beam pulse width is much extended by the neutral gas feed into the anode space.

§1. Introduction

A high density plasma has been widely used as an electron source of a high current electron gun. The maximum extractable currrent is limited by a space charge law. Then, to reduce a space charge limit, two usual methods are considered: One method is to reduce a distance between an extracting anode and a plasma surface. However, if a high extracting voltage is applied near a surface of the high density plasma source as shown in Fig.1(A), a breakdown is apt to generate between the beam extracting anode and the plasma source. Moreover, a large part of the electron beam current is lost into the extracting anode itself, because the extracting electric field is diverged around the central aperture. To avoid this breakdown and to concentrate the electron beam in the anode central aperture, the distance between the extracting anode and the plasma source must be sufficiently long. Then, the space charge limit becomes serious.

The other method is to introduce a neutral gas into the beam acceleration region as shown in Fig.1(B). The electron beam is neutralized with ions which are ionized by the beam electrons themselves. However, this electron beam becomes unstable through the ion loss and causes a discharge through an instability as has been pointed out already.[1] From another standpoint, a pulse width of a neutralized electron beam is limited by a back streaming time of ionized ions from the vicinity of the acceleration anode. Thus, an intense long pulsed electron beam has not been produced in this method.

We have reported a new method[2] to reduce the above

space charge limit stably and extract a "dc"-intense electron beam from a plasma source. In this paper, we will show that the new method is useful also to extract a "long pulsed"-intense electron beam, while principles of the new method are discussed more precisely than the previous report.

As another remarkable point in this paper, a high density plasma in a long pulse duration is produced with a fast rise time from a Ta hollow cathode discharge.[3,4] Usually, the hollow cathode is simple in the mechanism and strong against ion back stream damages in comparison with ordinary W wire cathodes or oxide cathodes. However, as the hollow cathode must be pre-heated, a discharge does not start with a fast rise time. Therefore, the hollow cathode discharge has not been used as a pulsed plasma source. We find an indirect pulse operation method on the hollow cathode.

§2. Principles of The Method

To reduce the space charge limit stably and to concentrate the accelerated electrons in the central aperture of the extracting anode, a new method is shown in Fig.2. (This principle has been reported already.[2]) In Fig.2, the anode region is expanded and a neutral gas is introduced locally. Then, in the anode region, ions are produced by accelerated electrons themselves through collisions with the neutral gas. The ionized ions stream backwards along the electric field. Here, if a pressure in a region between the anode A and source electrode S is adjusted in an optimum value, we can realize a state that collisions are negligible for electrons

and effective for ions. These relations for collisions are expressed by, if columb collisions are small,

$$\lambda_{en} >> L, \qquad \lambda_{in} \lesssim L, \tag{1}$$

where λ_{en}, λ_{in} and L are an electron-neutral, ion-neutral particle collision mean free path and a length between the anode A and the source electrode S. Thus, we may consider that the electron space charge is compensated by diffused back ground ions over all the accelerating space between A and S, while electrons are accelerated freely. Then, if a discharge does not occur between S and A, the accelerated electron beam current is limited by the initial plasma (thermal) electron current injected from the plasma sources. This means a temperature or flux limit. Then, the electron current is independent of the accelerating anode voltage. [By this characteristic on the accelerating voltage, we can divide an electron beam state in this flux limit from both ion and electron collisional type ($\lambda_{en} << L$ and $\lambda_{in} << L$) on from both ion and electron collisionless type ($\lambda_{en} >> L$ and $\lambda_{in} >> L$). In the case of both ion and electron collisional type, the electron current is proportional to the applied voltage. This case means a plasma resistance type. On the other hand, in the case of both ion and electron collisionless type, the electron current takes a space charge limit after $V^{3/2}$ for the anode applied voltage V. These three voltage characteristics are shown roughly in Fig.3.]

A pulse width Δt of an neutralized electron beam current is related to the neutralization time τ_i in a neutral gas and the ion loss time τ_ℓ in the electron beam. Here, the

neutralization time for the electron beam is determined from $n_i = P\,\eta\,(v_b)\,n_b\,v_b\,dt$, where n_i is an ion density ionized by the electron beam (it's density n_b, velocity v_b), P and $\eta\,(v_b)$ are a neutral gas pressure and the ionization probability (ion pairs per cm.Torr). The time dt expresses an ion build-up time in the electron beam while the ionized ions are "stationary". Thus, the neutralization time is defined by, as a time τ_i when n_i reahces n_b, that is, $dt(n_i = n_b) \equiv \tau_i$,

$$\tau_i = \frac{1}{P\eta(v_b)v_b} = \frac{1.7\times10^{-2}}{P\eta(V_b)V_b^{1/2}}\ , \qquad (2)$$

where V_b is an electron beam energy in eV unit, τ_i is measured by μsec and P is measured by Torr.

Obviously, the neutralization time τ_i gives a rise time for the pulsed electron beam current. On the other hand, the pulse width Δt of the current is limited by the ion loss time τ_ℓ from the electron beam. These relations are expressed by,

$$\tau_\ell > \Delta > \tau_i\ . \qquad (3)$$

In a case where a neutral gas is introduced directly as shown in Fig.1(B), the ion loss time is very short because of a back stream of ions.

However, in a case of the expanded anode space where the neutral gas is introduced, the ion loss time τ_ℓ in the acceleration space does not become important if the neutralization time τ_i in the expanded anode space is much below Δt. Because sufficient ions ionized by the electron beam itself stream backwards into the acceleration space from the expanded anode space. Then, the pulse width Δt is determined only by a pulse width of an injected plasma electron current.

Thus, the anode space is very important for the beam neutralization over a long pulse duration.

In the plasma source for the electron injection, we must determine a neutral gas pressure in which the initial electron flux $n_o v_o$ is larger. Moreover, if the plasma source is produced by a dc discharge, the discharge cathode must be protected from bombardments due to ions which back stream from the electron accelerating region. To avoid these ion bombardments by neutral particle collisions, both the neutral gas pressure and the plasma source length become important (as shown in Fig.2). That is, the pressure and the length of the plasma source must be determined from a maximum of $n_o v_o$ and the plasma source stability as reported already.[2)]

Under these principles, a schematic of the experimental apparatus in a dc operation is shown in Fig.4, which is the same with an apparatus in a pulse operation (described next) except S_2 electrode and external circuits. It is remarkable that the plasma source is produced from a hollow cathode discharge. A dc discharge is fired between a first anode S_1 and Ta pipe cathode K where a neutral gas is introduced through the pipe. Next, the secondary discharge is fired between S_1 and the second anode S_2 by a voltage on a load resistance R_L of S_1. Thus, a stable plasma is produced between S_2 and the third anode S_3 in a helium pressure of 10^{-2} Torr and a length of $\overline{S_2S_3}$ = 12 cm, while the pressure between K and S_1 is about 2 Torr and the pressure S_1 and S_2 is about 10^{-1} Torr. The characteristics of this apparatus are similar to the case of the oxide cathode as reported

already.[2] However, a more intense electron beam is produced easily under a Ta cathode which is much stronger than the oxide cathode. Up to now, we produce a dc intense electron beam in energy from 0.2 kV to 2.0 kV with a maximum 40 A in 0.8 cmϕ in a helium gas pressure 10^{-4} Torr.

Next, to extract a much more intense electron beam, this dc operation in the plasma source will be developed in a pulsed operation.

§3. Experimental Procedure

A schematic of the apparatus is shown in Fig.5. It should be remarkable that a pulse plasma source with a fast rise time (below 100 μsec) is produced from a cold cathode indirectly. A primary plasma source is produced by a dc hollow cathode discharge between an electrode S_1 (with a central aperture of 0.6 cmϕ in diameter and 2.5 cm in length) and a Ta pipe electrode K (0.6 cmϕ in outer diameter and 0.4 cmϕ in inner diameter). The gap between S_1 and K is about 1.0 cm. Usually, the dc hollow cathode discharge is kept with a discharge voltage 75 V and current 26 A(R_d = 2 Ω and $V_d \approx 127$ V) in a helium gas pressure of about 2 Torr. To stop the primary dc plasma flow into $\overline{S_2S_3}$ space, an electrode S_2(0.6 cmϕ in central aperture diameter and 8.0 cm in length) is put at a distance 10 cm apart from S_1. The pressure between S_1 and S_2 is about 10^{-1} Torr. A negative potential V_c through a resistance ($R_c \approx 20$ Ω) is applied betweeen S_1 and S_2. A pulsed plasma for electron injection is produced between S_2 and the third electrode S_3 (with 0.8 cmϕ in central aperture and 1.0 cm in length)

which is 12 cm apart from S_2. A pressure between S_2 and S_3 is kept at about 10^{-2} Torr, which is determined experimentally. Then, if the negative potential V_c between S_1 and S_2 is set at -80 V, the dc primary plasma electron flow into $\overline{S_2S_3}$ space is reduced below 20 mA by the neutral particle collisons and the retarding electric field of V_c.

Here, if a pulse potential above V_c is applied between S_1 and S_3 electrode by a charged condenser $C_s = 10^{-2}$ F through SCR, a pulsed secondary plasma is produced with a fast rise time (below 100 μsec) between S_2 and S_3, while the pulsed plasma electrons are injected between S_3 and an acceleration anode A_1. Then, to lead the secondary plasma from $\overline{S_1S_2}$ to $\overline{S_2S_3}$ space, a loading resistance $R_L \approx 0.5\ \Omega$ is connected to S_2. The pulsed plasma electron current between S_2 and S_3, and its pulse duration are adjusted by a charging voltage V_s for C_s and a capacitance of C_s.

The pulsed plasma electrons injected from $\overline{S_2S_3}$ space to $\overline{S_3A_1}$ space are accelerated by a potential of condenser $C_A = 9 \times 10^{-4}$ F which is charged by a dc power supply voltage V_A. Each space between K and S_1, S_1 and S_2, S_2 and S_3, or S_3 and A_1 is connected by a pyrex glass tube with a diameter of 10 cm. A length between S_3 and A_1 is 40 cm, where the helium gas pressure is kept within $(2.8 \sim 4.2) \times 10^{-4}$ Torr under the experimental results[2] in the dc operation.

Ion or electron mean free path of collisions in helium gas is estimated by, roughly, $\lambda_{in} \approx 2.0 \times 10^{-2}\sqrt{V_i}/P(cm)$ and $\lambda_{en} \approx 5.0 \times 10^{-2}\sqrt{V_e}/P(cm)$, where V_i, V_e and P are an ion, electron temperature in eV unit and a helium gas pressure

in Torr. For an experimental optimum pressure $P \approx 4.0 \times 10^{-4}$ Torr, we obtain $\lambda_{in} \approx 5.0 \times 10\sqrt{V_i}$(cm) and $\lambda_{en} \approx 1.3 \times 10^2$ $\sqrt{V_e}$(cm). The ion temperature or the electron temperature in the plasma injected into A_1S_3 region is estimated to be $V_e \gtrsim 10$ eV and $V_i \lesssim 0.5$ eV from data in the dc operation. Thus, we can estimate $\lambda_{en} \gtrsim 4 \times 10^2$ cm and $\lambda_{in} \lesssim 3.5 \times 10$ cm. These mean free paths are compared with the distance $\overline{A_1S_3} \simeq$ 40 cm under the experimental principle "electron collisionless and ion collisional". A helium gas is introduced between acceleration electrodes A_1 and A_2 where the pressure is varied from 2.1×10^{-4} to 3.5×10^{-3} Torr experimentally. The distance between A_1 and A_2 is 16 cm, which is very important for the electron beam stability as reported already.[2] The A_1 or A_2 electrode is 6 cm or 5 cm in length and has a central aperture of 1.6 cmϕ or 1.4 cmϕ.

Under the most optimum experimental conditions, a large part of the accelerated electron beam is collected through $\overline{A_1A_2}$ region to an electrode A_3 (given a potential equal to A_1 or A_2 by a charged condenser $C_B = 1.8 \times 10^{-3}$ F). The pressure in $\overline{A_2A_3}$ region is kept around 10^{-4} Torr. Through a small resistance $R = 0.1\ \Omega$, the electron beam current to the final electrode A_3 is measured by setting a switch SW on position 1, while the total beam current to all anode electrodes (A_1, A_2 and A_3) is measured by turning the SW on position 2.

A magnetic field B is applied uniformly at B = 1.3 K gauss from A_3 to S_2. However, the magnetic field is diverged from S_2 to K and is set at B = 300 gauss on S_1 to stabilize

the primary dc discharge.

§4. Experimental Results

Dependence of the electron beam current ($I_{B1} \equiv I_b$) to A_3 on the pressure P_A between A_1 and A_2 is shown in Figs. 6(A) - 6(F) under an accelerating voltage V_A = 400 V and the plasma source secondary discharge voltage V_s = 280 V. Then, a voltage on the condenser C_B is monitored, which stays within 5/6 of V_A. We find that the pressure P_A must be above 7.0×10^{-4} Torr to produce a large electron beam current above 100 A. Then, the electron beam is produced with a fast rise time below 100μsec and a long decay time 2 msec.

Dependence of the electron beam current I_b on the accelerating voltage V_A is shown in Figs. 7(A) - 7(D) under $P_A = 1.4 \times 10^{-3}$ Torr. The electron beam current hardly depends on V_A (for above 200V).

The "electron beam mode" is divided from a "discharge mode" by monitoring a total anode current ($I_{B2} \equiv I_B$) (to A_1, A_2 and A_3) and a voltage on condenser C_A or C_B. In the discharge between S_3 and the anodes (A_1, A_2 or A_3), the voltage on C_B or C_A drops abruptly as shown in Fig.8 under V_A = 660 V, $P_A = 2.0 \times 10^{-3}$ Torr, and V_s = 280 V, while a current to anode A_3 much exceeds the plasma source current I_s. In the electron beam extraction, a current conservation among the total current I_B to the accelerating anodes (A_1, A_2 and A_3), the plasma source current I_s and a current ΔI_s through the loading resistance R_L, is seen. That is, as

seen from Fig.9

$$I_s = I_B + \Delta I_s \ . \qquad (4)$$

For V_A = 400 V, V_s = 280 V and $P_A = 1.4 \times 10^{-3}$ Torr, we find for the maxima that I_s = 800 A, $\Delta I_s \approx$ 400 A and I_B = 400 A as seen in Figs. 9(A), (B) and (C). A ratio I_b/I_B between the electron beam current I_b to A_3 and the total current I_B to the all anodes shows a beam concentration rate in the central apertures of A_1 and A_2. For the optimum pressure P_A, the beam concentration I_b/I_B is up to 0.8 as seen in Figs. 9(B) and (C). On the other hand, if the neutral gas is not fed between A_1 and A_2, the ratio I_b/I_B is below 0.2 as seen from Fig.6(A).

For $P_A > 3.5 \times 10^{-3}$ Torr and $V_s >$ 350 V, a discharge between S_3 and anodes (A_1, A_2 or A_3) is apt to start. Under the present experimental conditions, an intense electron beam with a maximum energy 1 kV and a maximum current 0.8 kA is produced in an exponential decay time 2 msec when V_s = 350 V and $P_A \approx 1.0 \times 10^{-3}$ Torr.

Under V_A = 400 V, V_s = 280 V and $P_A = 1.4 \times 10^{-3}$ Torr, the plasma wall potential in the accelerating region between S_3 and A_1 is investigated radially by a probe P_r which is put in the middle point between S_3 and A_1. Figs. 10(A) and (B) show each potential near the tube wall ($r \approx$ 4.5 cm) or near the center ($r \approx$ 0.5 cm). Then, the voltage on the accelerating anode A_1 is monitored in Fig.10(C). It should be remarkable that the potential near the tube wall is much higher than a potential of the anode A_1, and that the

potential near the center is much below the potential of A_1.

§5. Discussion

It is considered that an electron beam is produced under an initial flux limit from the following experimental results: a nearly constant characteristic of the beam current on the accelerating voltage V_A and a linear potential increment from the plasma source electrode S_3 to the first anode A_1. A large difference between the beam mode and the discharge mode in $\overline{A_1 S_3}$ region is on the voltage drop of condenser C_A or C_B also. In a flux limit electron beam, a capacitance of condenser C_A sufficient to accelerate the electron beam in a constant energy, is determined from a beam equivalent resistance R_b and an initially injected electron current $(I_s - \Delta I_s) \approx I_B$. The R_b is defined by $R_b \approx V_b/I_B$, while V_b is a beam accelerating potential and is approximated by $V_b = V_A \exp(- t/C_A R_b)$. On the other hand, the injected plasma electron current $(I_s - \Delta I_s) \approx I_B$ is experimentally observed by $I_B \approx I_o \exp(- t/C_s R_s)$ where I_o and R_s are an initial beam current after the rise time and a plasma source effective resistance. From these equations, we obtain

$$\begin{aligned} V_b(t) &= V_A \exp(- t/\tau_{eff}) \\ \tau_{eff} &= C_A(V_b/I_o)\exp(t/C_s R_s) \\ &\approx C_A(V_A/I_o) \exp(t/C_s R_s) \ . \end{aligned} \tag{5}$$

Thus, an effective time constant τ_{eff} of the voltage drop

on C_A is much extended by a factor of $\exp(t/C_sR_s)$ which increases temporally. The maximum R_s is estimated by $R_s \approx 0.3\ \Omega$ from the plasma source current I_s and the charging voltage V_s. Experimentally, the voltage on C_A is sustained above 5/6 of V_A over a long pulse duration of the electron beam under $C_A \approx 9 \times 10^{-4}$ F, $C_B = 1.8 \times 10^{-3}$ F, $V_A = 400$ V, $I_o \approx 400$ A and $V_s = 280$ V. It is noted that pulse forming networks are not necessary if the electron beam current decays exponentially.

In a discharge mode between the anodes (A_1, A_2 and A_3) and S_3, the voltages on C_A and C_B drop abruptly since the effective discharge resistance is very small (below 0.02 Ω) compared with the beam resistance (above 1.0 Ω). The discharge current (~ 2 kA) much exceeds the injected current (~ 0.4 kA) from the plasma source. Therefore, the current conservation is not found.

In relation with a pulse width of the extracted electron beam, an neutralization time τ_i in the expanded anode space $\overline{A_1A_2}$ is important, which is estimated in Eq.(2) already. In a case of no gas introduction into $\overline{A_1A_2}$, the neutralization time is above 10 μsec since $P_A \lesssim 2 \times 10^{-4}$ Torr, $V_b \approx V_A = 400$ V and $\eta(V_b) \approx 1.0$ in Eq.(2). (Obviously, if the $\overline{A_1A_2}$ space is zero, the anode space is determined only by the $\overline{A_2A_3}$ space where the pressure is much lower than P_A, and τ_i is extended above 100 μsec.) If the helium gas pressure in the expanded anode $\overline{A_1A_2}$ space increases to $P_A = 1.4 \times 10^{-3}$ Torr (an optimum pressure) by introducing a secondary helium gas from a port in $\overline{A_1A_2}$, the neutralization time τ_i is reduced

below 1 μsec.

A loss time τ_ℓ of the ionized ions along the magnetic field B is estimated by, if the radial loss time is longer sufficiently compared with the loss time along B,

$$\tau_\ell = x/v_i \ . \tag{6}$$

where x is a distance along B and v_i is an ion speed. In the anode region $\overline{A_1A_2}$, we may take $x = \overline{A_1A_2} \approx 16$ cm and $v_i \approx 7.5 \times 10^5\sqrt{V_i}$ cm/sec for He^+ ion. Then, if we assume $V_i \approx 1$ eV (thermal), we obtain $\tau_\ell(\overline{A_1A_2}) \approx 20$ μsec. In the accelerating region $\overline{A_1S_3}$, we should take $x \approx \Delta\ell$ (electron sheath length near the acceleration anode A_1) and $v_i \approx 7.5 \times 10^5\sqrt{V_A}$ cm/sec, where V_A is the anode voltage which accelerates ions backwards. For $V_A \approx 400$ V and $\Delta\ell << \overline{A_1S_3} = 40$ cm, we obtain $\tau_\ell(\overline{A_1S_3}) << 3$ μsec. A neutralization time $\tau_i(\overline{A_1S_3})$ in the acceleration region near the anode A_1 is $\tau_i(\overline{A_1S_3}) \approx 3$ μsec for 3.0×10^{-4} Torr and $V_A = 400$ V. Thus, we can estimate $\tau_i(\overline{A_1A_2}) > \tau_\ell(\overline{A_1A_2}) > \tau_i(\overline{A_1S_3}) >> \tau_\ell(\overline{A_1S_3})$ in a case of no gas introduction. That is, in the $\overline{A_1S_3}$ region, ionized ions are lost quickly and supplied slowly. This means a space charge limit. Experimentally, in a case of no gas introduction, a large electron beam current is not extracted as seen in Fig.6(A).

Obviously, for $P_A = 1.4 \times 10^{-3}$ Torr (in a case of gas introduction into $\overline{A_1A_2}$), we can estimate $\tau_i(\overline{A_1A_2}) << \Delta t$ (pulse width) and $\tau_i(\overline{A_1A_2}) << \tau_\ell(\overline{A_1A_2})$. Therefore, by a back stream of ions from the $\overline{A_1A_2}$ region to the $\overline{A_1S_3}$, the space charge of electron sheath is compensated quickly.

Thus, a large electron beam current is extracted up to the injected plasma source electron current (a flux limit) as seen from Figs. 6(C), (D) and (E).

Next, in the relation with the beam energy spread, the beam electron energy loss in $\overline{A_1A_2}$ region must be estimated. Then, the beam energy loss is about 1 eV under $P \approx 1.4 \times 10^{-3}$ Torr and $V_A = 400$ V, which is neglected for the beam energy. In the dc operation as shown in Fig.4, if the pressure in $\overline{A_1A_2}$ is below 1.4×10^{-3} Torr, we find that the beam energy spread $\Delta V_b/V_b$ in the final space ($\overline{A_2A_3}$) is below 20 % for a beam energy $V_b > 200$ V.

In the accelerating region ($\overline{A_1S_3}$), a potential near the tube wall is much above the acceleration voltage of A_1 electrode. The fact may be due to high energy ions which stream backwards from the anode region $\overline{A_1A_2}$ as reported[2] in the dc operation already. The high energy ions may be scattered by the injecting cold ions through ion-ion collisions since the ion density is above 10^{12}/cc in the present experimental conditions. On the other hand, obviously, the electron-ion collision mean free path is much longer than the accelerating region distance $\overline{A_1S_3}$. Thus, for the coulomb collisions, we may assume that electrons are collisionless and ions are collisional in $\overline{A_1A_3}$ space.

We can expect a higher beam energy by increasing V_A, a larger beam current by increasing V_s and the primary dc discharge current I_d, and a longer pulse duration by increasing C_S, C_A and C_B under an optimum gas introduction into $\overline{A_1A_2}$ region.

In conclusion, by introducing a neutral gas into an expanded anode space, a long pulsed intense electron beam highly concentrated in the anode central aperture, is extracted from a pulsed plasma source which is based on a dc hollow cathode discharge, but has a fast rise time.

Acknowledgement

I wish to thank Dr. K. Akaishi for valuable comments.

References

1. M. V. Nezlin, Zh. Eksp. Teor. Fiz. 41, 1015 (1961); Sov. Phys. JETP 14, 723 (1962)
2. J. Uramoto, Research Report of Institute of Plasma Physics, Nagoya University, Nagoya, Japan, IPPJ-237 (1975)
3. L. M. Lidsky et al., J. Appl. Phys. 33, 2490 (1962)
4. S. Komiya and K. Tsuruoka, J. Vac. Sci. Technol. 12 589 (1975)
5. E. G. Linder and K. G. Hernqvist, J. Appl. Phys. 21, 1088 (1950)

Figure Captions

Fig.1(A) Ordinary Electron Sheath Method.

A: Acceleration anode. d: Central aperture.

Δx: Electron sheath. E: Electric field.

(B) Direct Gas Introduction Method.

I_s: Plasma thermal electron current

I_b: Electron beam current

Fig.2 New Method (Principle of Stable Neutralization).

A: Expanded acceleration anode. S: Plasma source anode. I_s: Thermal plasma electron current. I_b: Electron beam current. E: Electric field.

Fig.3 General dependences of electron current I in plasma on applied voltage V.

(1) : Plasma Resistance Type (Both electron and ion collisonal).

(2) : Initial Flux Limit Type (Electron collisionless, but ion collisional).

(3) : Space Charge Limit Type (Both electron and ion collisionless).

Fig.4 Schematic of experimental apparatus in dc operation.

S_2: Plasma source second anode (8 mmϕ in central aperture dia. and 8.0 cm in length).

[except S_2 and external circuits, same in Fig.5], see Fig.5.

Fig.5 Schematic of experimental apparatus in pulse

operation.

K: Ta pipe cathode. S_1: Plasma source first anode. S_2 Plasma source second anode. S_3: Plasma source third anode. A_1: Acceleration first anode. A_2: Acceleration second anode. A_3: Acceleration third anode (Faraday Cup). B: Magnetic field. R: Charging resistance (500 Ω).

Fig.6 Dependence of electron beam current I_b (to anode A_3) and acceleration voltage V_b (voltage on A_3) on anode pressure P_A (between A_1 and A_2 anode). t: time 500 μsec/div. I_b: 100 A/div. V_b: 133 V/div.

V_A = 400 V (voltage charging C_A and C_B).

V_S = 280 V (voltage charging C_S).

(A) : $P_A \leq 2.1 \times 10^{-4}$ Torr. (B) : $P_A = 7.0 \times 10^{-4}$ Torr. (C) : $P_A = 1.4 \times 10^{-3}$ Torr. (D) : $P_A = 2.1 \times 10^{-3}$ Torr. (E) : $P_A = 3.5 \times 10^{-4}$ Torr.

Fig.7 Dependence of electron beam current I_b on acceleration anode voltage V_A (charging voltage on C_A and C_B).

I_s: Plasma source current (between S_1 and S_3 electrode), 400 A/div. I_b: 100 A/div. t: time 500 μsec/div. V_s = 280 V. $P_A = 1.4 \times 10^{-3}$ Torr (between A_1 and A_2). (A): V_A = 100 V. (B): V_A = 200 V. (C): V_A = 300 V. (D): V_A = 660 V.

Fig.8 Discharge mode (between source electrode S_3 and all acceleration anodes A_1, A_2, A_3).

I_{A3}: Discharge current to A_3, 400 A/div. V_{A3}: Voltage on A_3, 220 V/div. t: time 500 μsec/div. $P_A = 1.6 \times 10^{-3}$ Torr. $V_A = 660$ V. $V_S = 280$ V.

Fig.9 Current conservation between plasma source currents and electron beam currents.

I_S: A plasma source (total) current between S_1 and S_3, 400 A/div.

ΔI_S: A plasma source (by-pass) current between S_1 and S_2, 200 A/div.

t: time 500 μsec.

I_B: A total electron current (to A_1, A_2 and A_3), 100 A/div.

I_b: Electron beam current (to A_3), 100 A/div.

$V_A = 400$ V, $V_S = 280$ V, $P_A = 1.4 \times 10^{-3}$ Torr.

Fig.10 Potential Distribution.

I_b: Electron beam current, 100 A/div. V_p: Plasma wall potential, 133 volt/div. t: time 500 μsec.

V_{A1}: Voltage on electrode A_1. $V_S = 280$ V.

$P = 1.4 \times 10^{-3}$ Torr. $V_A \approx 400$ V.

(A) : Plasma wall potential near tube wall.

(B) : Plasma wall potential near center.

(C) : Potential of acceleration electrode A_1.

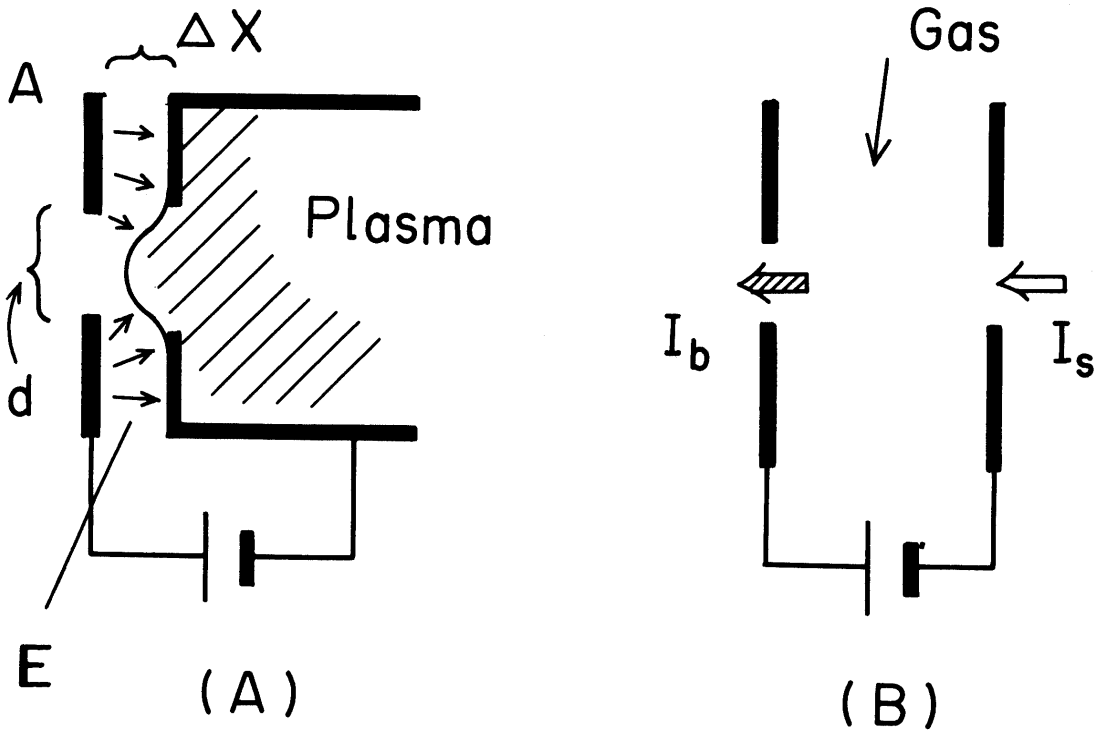

Fig. 1

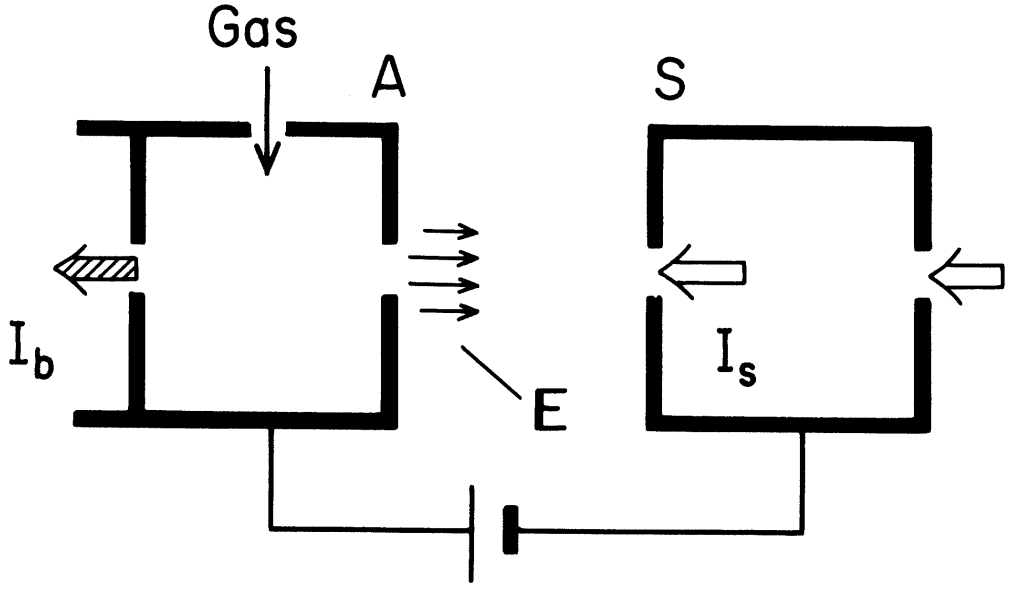

Fig. 2

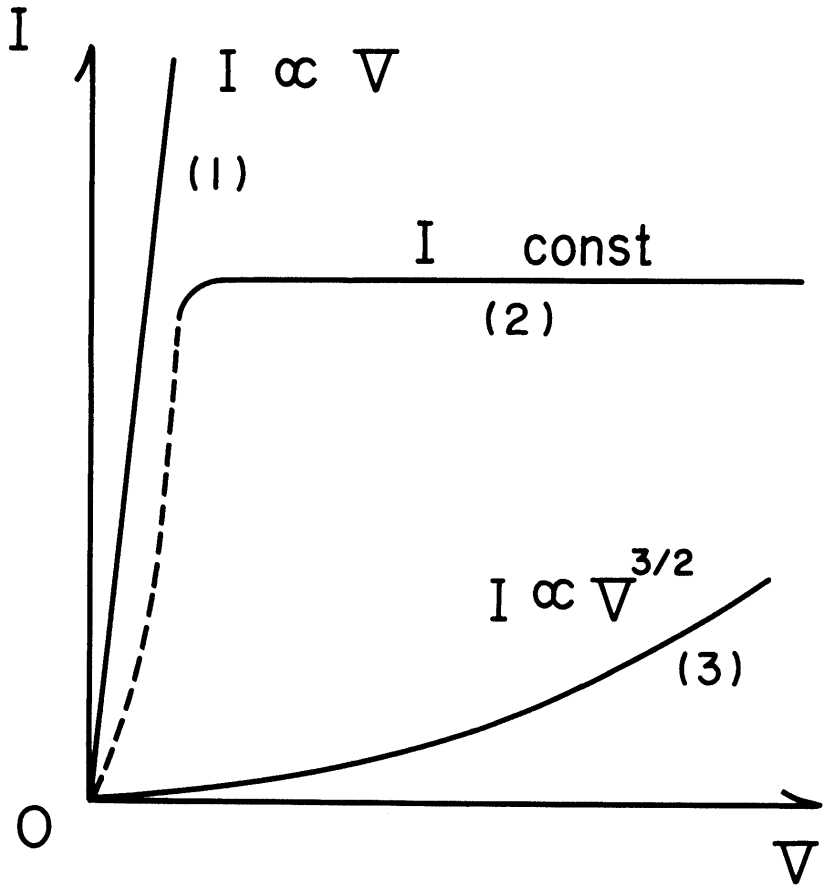

Fig. 3

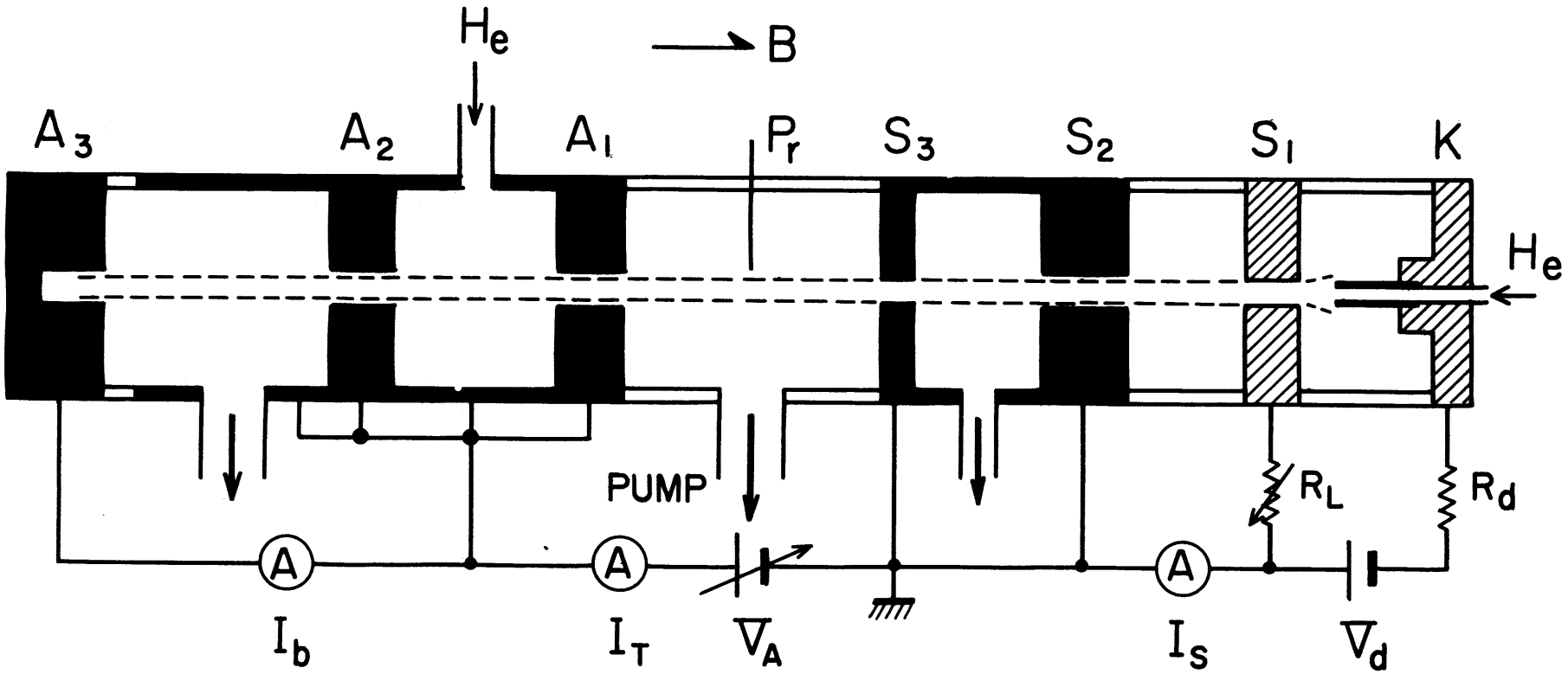

Fig. 4

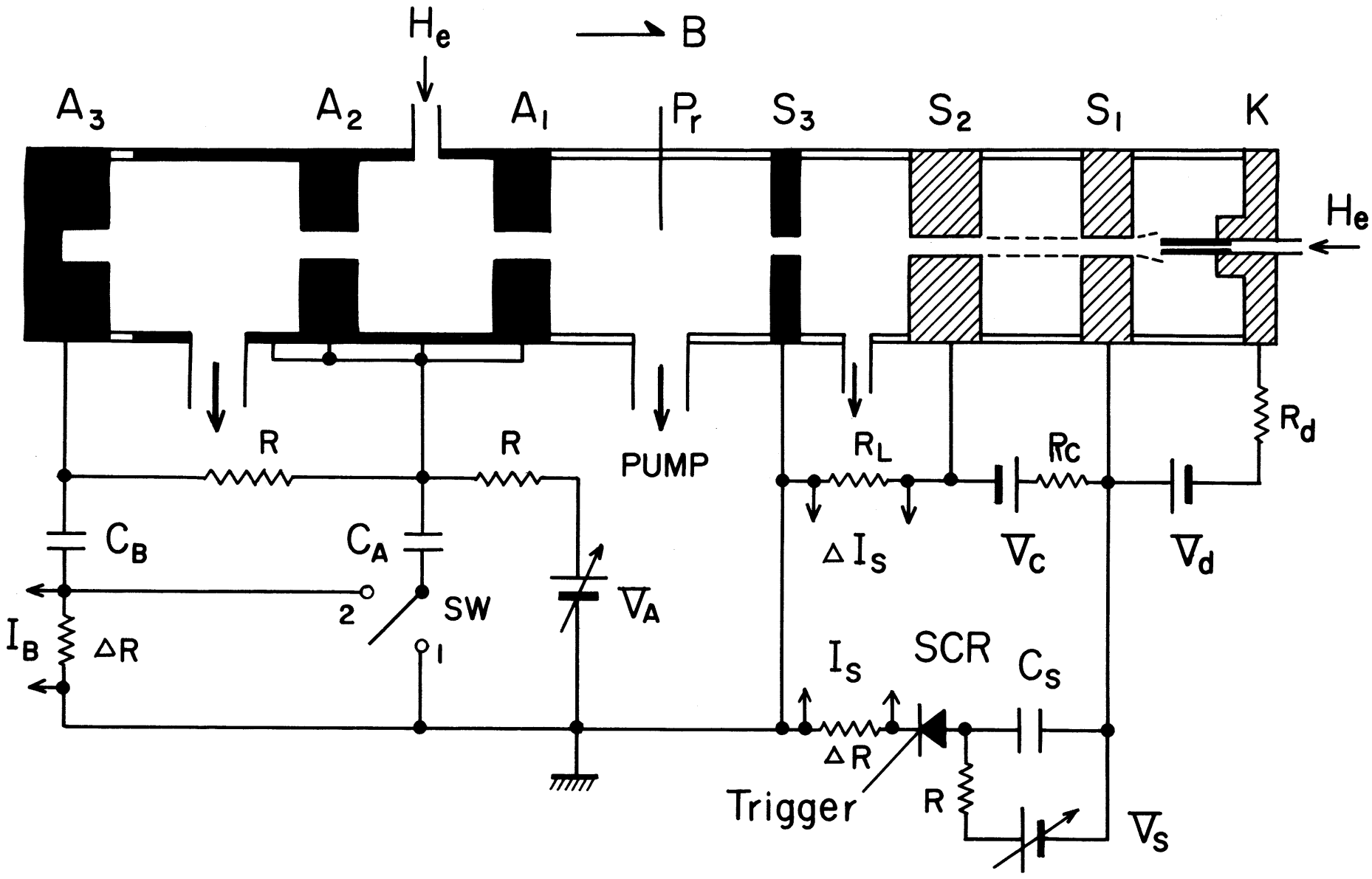
He
B
A3
A2
A1
Pr
S3
S2
S1
K
He
R
R
PUMP
RL
Rc
Rd
CB
CA
SW
2
1
VA
ΔIs
Vc
Vd
IB
ΔR
Is
SCR
Cs
ΔR
Trigger
R
Vs

Fig. 5

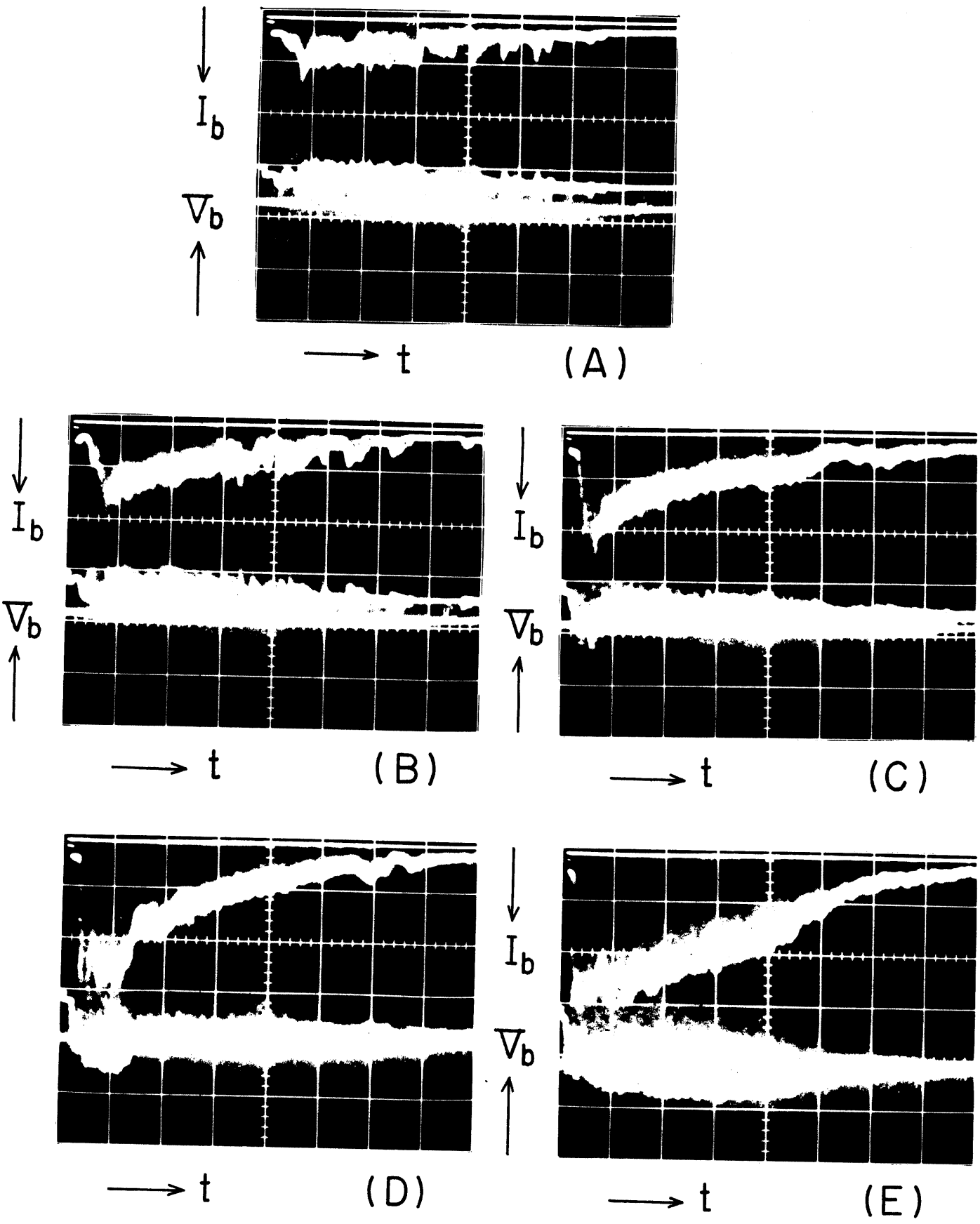

Fig.6

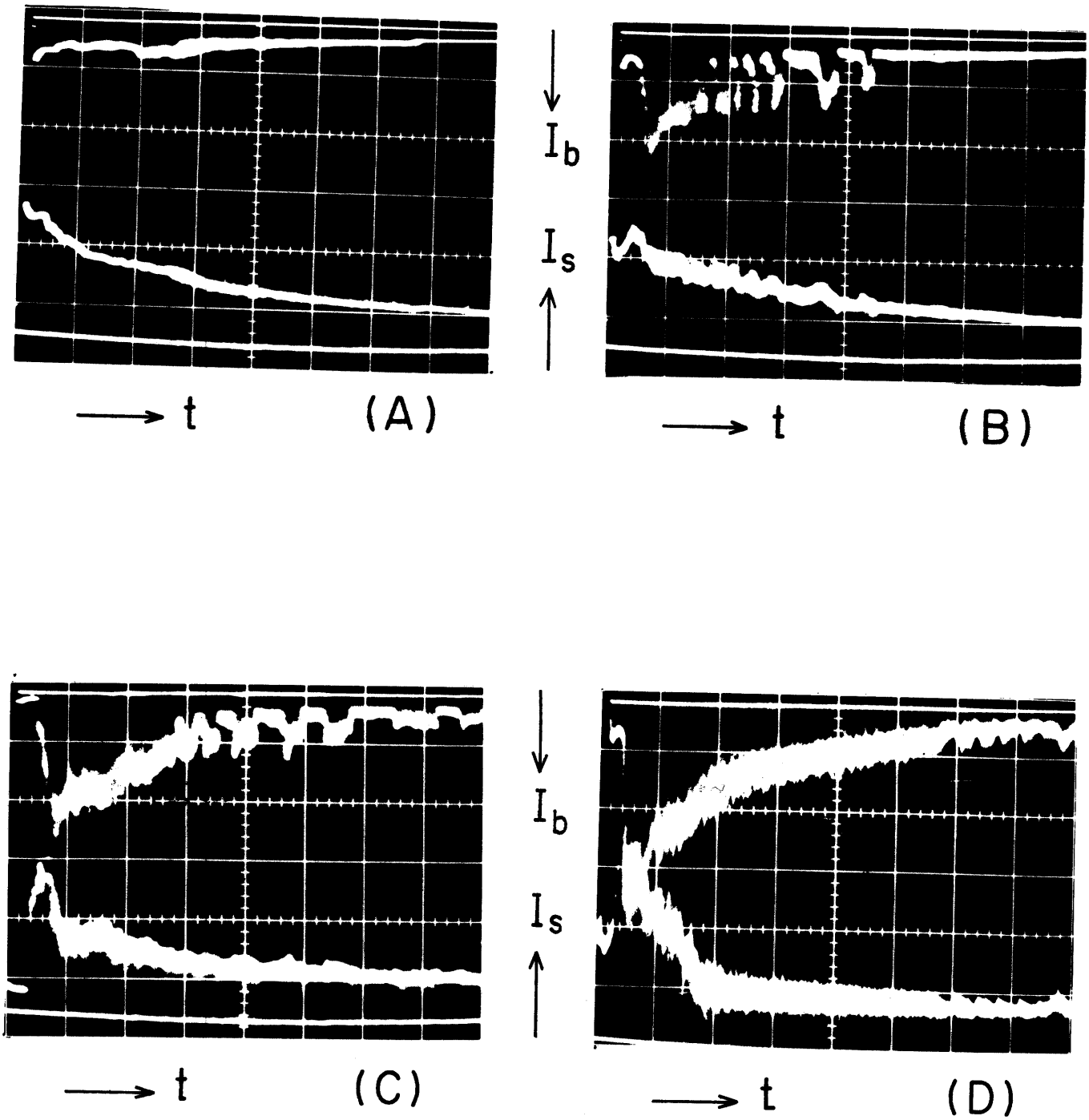

Fig. 7

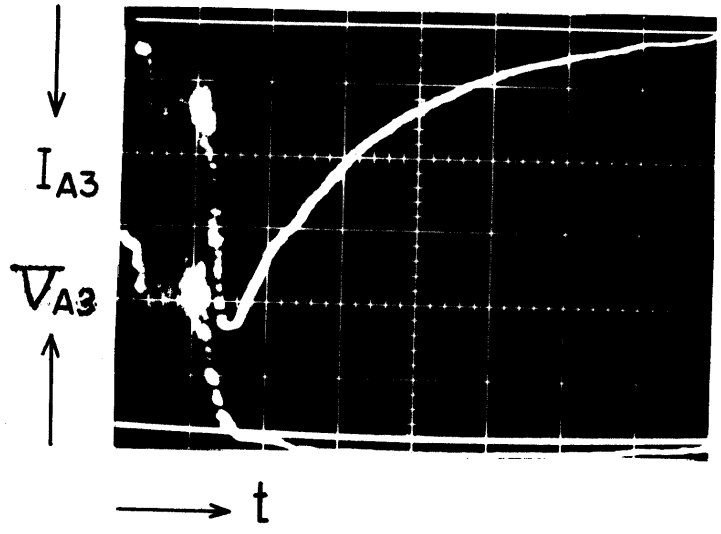

Fig.8

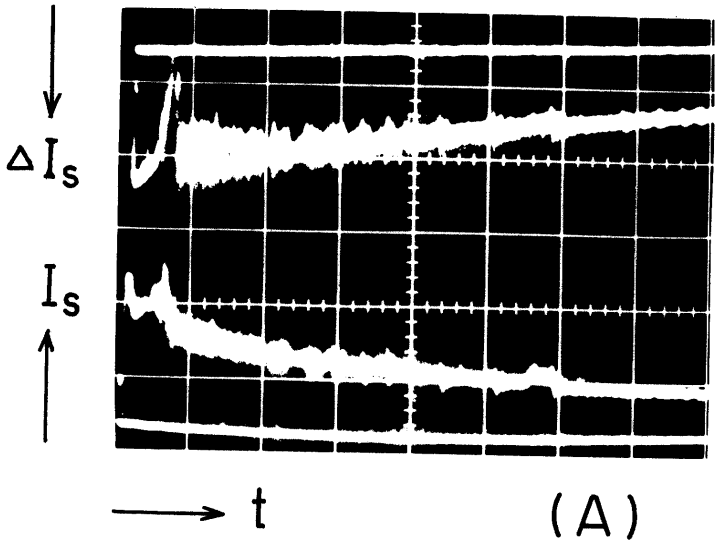

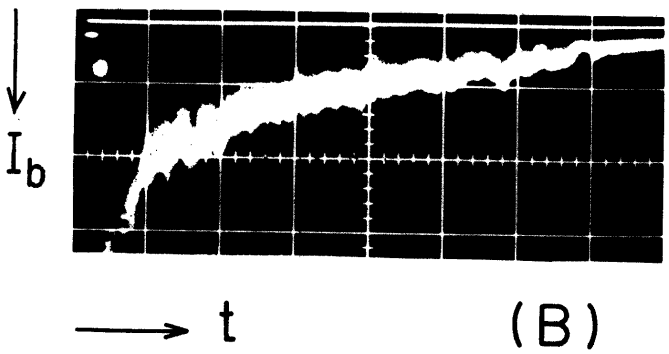

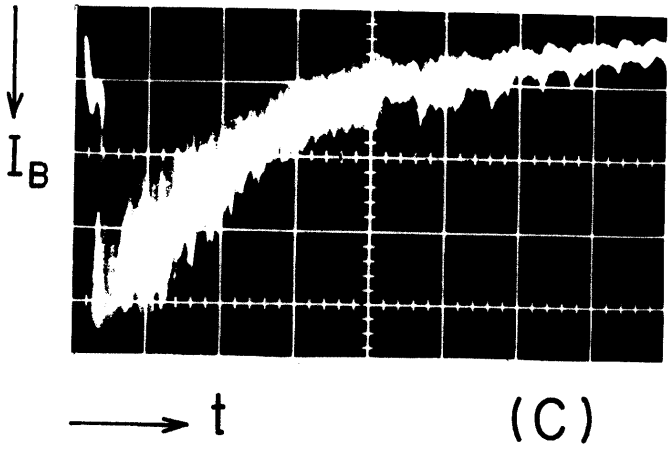

Fig.9

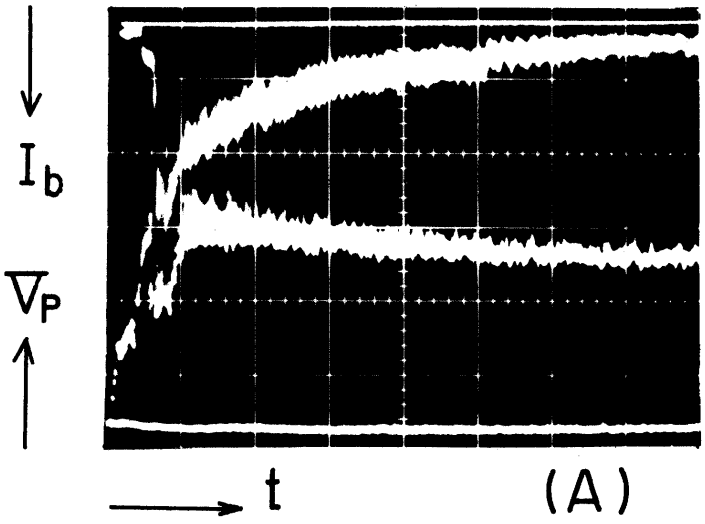

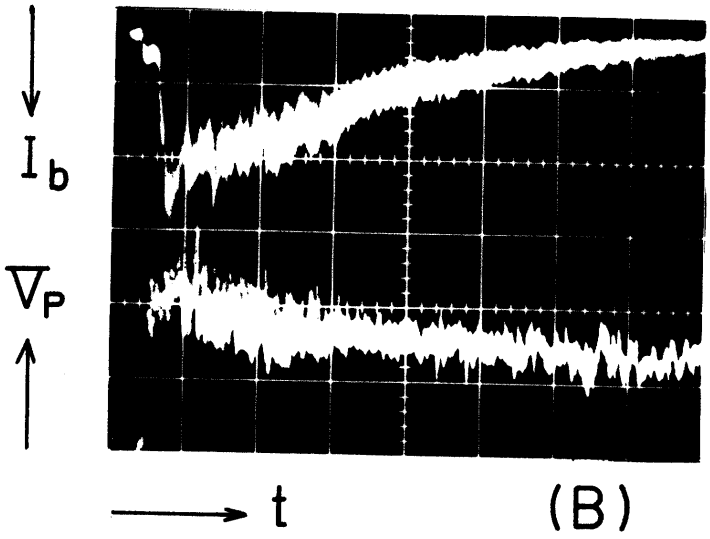

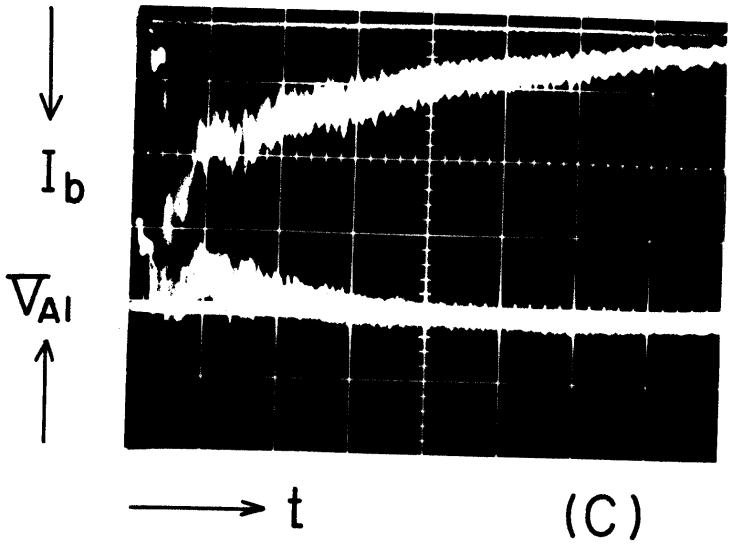

Fig.10